



Supplement of

Giant dust particles at Nevado Illimani: a proxy of summertime deep convection over the Bolivian Altiplano

Filipe G. L. Lindau et al.

Correspondence to: Filipe G. L. Lindau (filipelindau@hotmail.com)

The copyright of individual parts of the supplement might differ from the article licence.

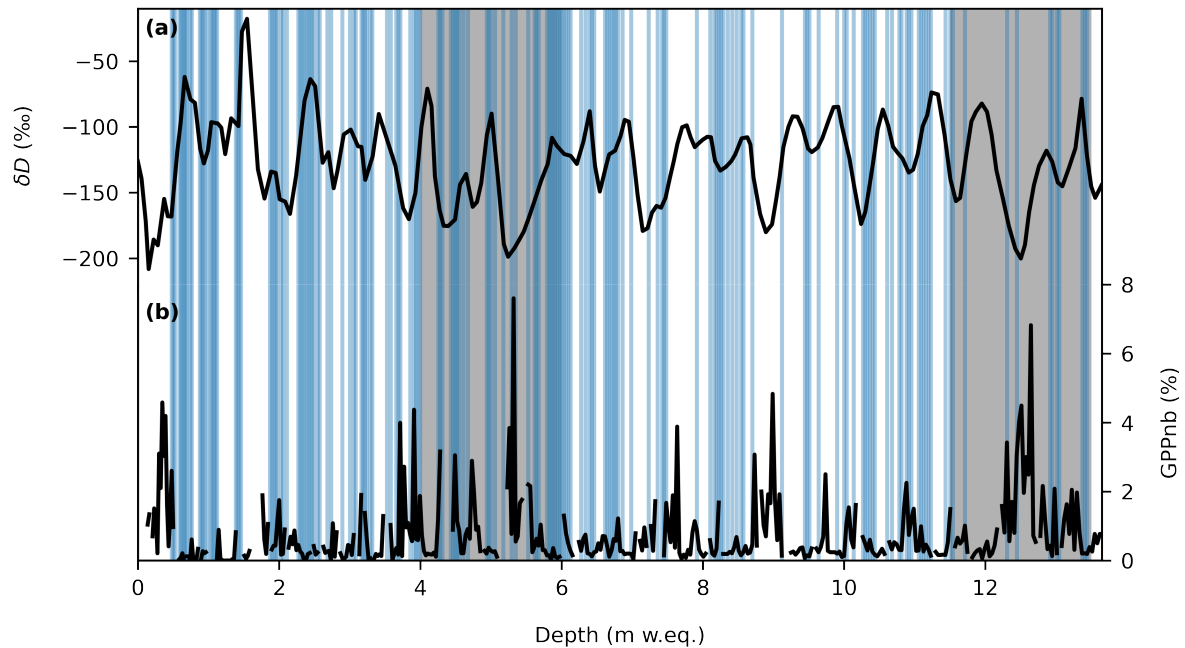


Figure S1. Ice and/or crust layers recorded in the Illimani's firn core (blue vertical lines) along with the records of δD (a) and GPPnb (b). The gray area in the depth range 4–6 mw.eq. features more ice/crust layers than the gray area within the 11.5–13.5 mw.eq. interval. However, both the variability in (a) and (b) show no evidence of signal change due to the occurrence of these layers.

Table S1. Sections of the Nevado Illimani firn core analysed for elemental (N1 to N10) and mineralogical (R1 to R4) composition.

Sample	N1	N2	N3	N4	N5	N6	N7	N8	N9	N10	R1	R2	R3	R4
Top depth (m)	1.67	2.31	5.57	8.67	10.56	13.60	13.69	19.10	20.29	21.41	5.79	5.91	9.80	10.00
Bottom depth (m)	2.31	3.78	7.02	8.97	11.66	13.69	14.78	19.25	20.48	22.50	5.82	6.00	9.84	10.17

Table S2. Average elemental concentrations measured by Instrumental Neutron Activation Analysis, and the procedural errors and detection limits (DL). For comparison, we also present mean concentrations of dust particles from high elevation ice cores in the Alps (Thevenon et al., 2009) and in Tibetan plateau (Wu et al., 2009).

Element	Ce	Cs	Eu	Hf	La	Sc	Sm	Th	Yb
Concentration (ppm)	89.8	21.1	1.6	13.1	40.8	13.7	8.14	17.6	2.71
Error (%)	7.24	13.8	6.65	9.97	4.05	3.97	7.27	7.16	10.8
DL (ppm)	7	4	0.8	3	0.5	0.3	0.1	4	0.1
Colle Gnifetti ice core, Alps (ppm)	1.76	1.20	1.78	5.24	2.74	18.6	4.63	3.49	6.25
Dunde ice core, Tibetan Plateau (ppm)	65.7		1.09	4.04	32.6		5.51	14.3	2.93

Table S3. Mineral phases and relative abundance (number of grains, %) in Illimani firn from different time periods.

	R1	R2	R3	R4
Year	2010	2009–10	2004–05	2004
Season	dry	wet	wet	dry
Particles analyzed	167	161	138	167
	N (%)	N (%)	N (%)	N (%)
Quartz and polymorphs	31.7	21.7	13.8	23.4
K-feldspars	7.2	10.6	5.1	11.4
Plagioclases	10.8	9.3	7.2	18.6
Muscovite-illite-smectite	23.4	29.2	59.4	19.2
Other phyllosilicates	0.6	1.2	0	1.2
Clay minerals (kaolinite)	0.6	1.2	0	3
Clinopyroxenes	0	0.6	0	0
Orthopyroxenes	0	0	0	0
Amphiboles	0	0	0	0
Rutile	2.4	2.5	0	0.6
Anatase	4.2	6.8	4.3	2.4
Hematite	9	8.7	7.2	14.4
Goethite	8.4	5.6	1.4	3
Carbonates	0	1.2	0	0
Epidotes	0	0	0	0
Titanite	0	0	0	0
Tourmaline	1.2	0	0.7	0.6
Other heavy minerals	0.6	1.2	0.7	1.2
Other light minerals	0	0	0	1.2
Total	100	100	100	100

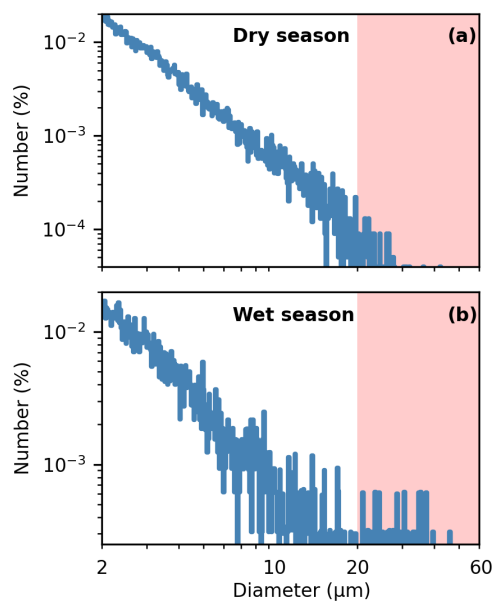


Figure S2. The number size distribution of a typical sample from the (a) dry and (b) wet season. Red areas highlight the giant particles (between 20 and 60 μm)

References

- Thevenon, F., Anselmetti, F. S., Bernasconi, S. M., and Schwikowski, M.: Mineral dust and elemental black carbon records from an Alpine ice core (Colle Gnifetti glacier) over the last millennium, *Journal of Geophysical Research Atmospheres*, 114, 1–11, <https://doi.org/10.1029/2008JD011490>, 2009.
- Wu, G., Zhang, C., Gao, S., Yao, T., Tian, L., and Xia, D.: Element composition of dust from a shallow Dunde ice core, Northern China, *Global and Planetary Change*, 67, 186–192, <https://doi.org/10.1016/j.gloplacha.2009.02.003>, 2009.